

# Low-Energy Excitations in Quantum Spin-Liquids Identified by Optical Spectroscopy

A. Pustogow,<sup>1</sup> Y. Saito,<sup>1,2</sup> E. Zhukova,<sup>1,3</sup> B. Gorshunov,<sup>1,3</sup> R. Kato,<sup>4</sup> T.-H. Lee,<sup>5</sup> V. Dobrosavljević,<sup>5</sup> and M. Dressel<sup>1</sup>

<sup>1</sup>*Physikalisches Institut, Universität Stuttgart, Pfaffenwaldring 57, D-70550 Stuttgart Germany*

<sup>2</sup>*Department of Physics, Hokkaido University, Sapporo, Japan*

<sup>3</sup>*Moscow Institute of Physics and Technology (State University), 141700, Dolgoprudny, Moscow Region, Russia*

<sup>4</sup>*RIKEN, 2-1, Hirosawa, Wako-shi, Saitama 351-0198, Japan*

<sup>5</sup>*Department of Physics and National High Magnetic Field Laboratory, Florida State University, Tallahassee, Florida 32306, USA*

(Dated: March 11, 2019)

The electrodynamic response of organic spin liquids with highly-frustrated triangular lattices has been measured in a wide energy range. While the overall optical spectra of these Mott insulators are governed by transitions between the Hubbard bands, distinct in-gap excitations can be identified at low temperatures and frequencies which we attribute to the quantum spin liquid state. For the strongly correlated  $\beta'$ -EtMe<sub>3</sub>Sb[Pd(dmit)<sub>2</sub>]<sub>2</sub>, we discover enhanced conductivity below 175 cm<sup>-1</sup>, comparable to the energy of the magnetic coupling  $J \approx 250$  K. For  $\omega \rightarrow 0$  these low-frequency excitations vanish faster than the charge-carrier response subject to Mott-Hubbard correlations, resulting in a dome-shape band peaked at 100 cm<sup>-1</sup>. Possible relations to spinons, magnons and disorder are discussed.

PACS numbers: 75.10.Kt 71.30.+h, 74.25.Gz 78.30.Jw

Quantum spin liquids are an intriguing state of matter [1–4]: although the spins interact rather strongly, the combination of geometrical frustration and quantum fluctuations prevents long-range magnetic order even in two and three dimensions. It took decades before clear experimental realizations of this theoretical concept [5, 6] became available, first in the organic compound  $\kappa$ -(BEDT-TTF)<sub>2</sub>Cu<sub>2</sub>(CN)<sub>3</sub>, which crystallizes in a triangular pattern [7], and later in the kagome lattice of ZnCu<sub>3</sub>(OH)<sub>6</sub>Cl<sub>2</sub> [8–10]. Despite this progress, a smoking gun experiment identifying its essential features is still lacking, and even a reliable theoretical description of real spin liquid systems remains a subject of much controversy and debate. At present, the fundamental nature of the spin-liquid state is far from being understood.

Herbertsmithite (ZnCu<sub>3</sub>(OH)<sub>6</sub>Cl<sub>2</sub>) is a layered anti-ferromagnetic insulator with no magnetic order above 50 mK. Inelastic neutron scattering experiments did not find indications of a spin gap down to 0.1 meV, inferring that the spin excitations form a continuum [2]. This important issue, however, is far from being settled neither from the experimental nor from the theoretical side [11, 12]. Among other suggestions [13–17], it was proposed that a gapless U(1) spin-liquid state forms with a spinon Fermi surface and with a Dirac-fermion excitation spectrum of the kagome lattice [18, 19].

The situation might become clearer by considering the charge-transfer salts  $\kappa$ -(BEDT-TTF)<sub>2</sub>Cu<sub>2</sub>(CN)<sub>3</sub> (abbreviated CuCN, BEDT-TTF denotes bis(ethylenedithio)-tetrathiafulvalene),  $\kappa$ -(BEDT-TTF)<sub>2</sub>Ag<sub>2</sub>(CN)<sub>3</sub> (called AgCN) and  $\beta'$ -EtMe<sub>3</sub>Sb[Pd(dmit)<sub>2</sub>]<sub>2</sub> (short EtMe, dmit is 1,3-dithiole-2-thione-4,5-dithiolate); here the molecular dimers with spin- $\frac{1}{2}$  form a highly frustrated triangular lattice [7, 20–22]. At ambient pressure no indication of Néel order is observed at temperatures as low as 20 mK,

despite the considerable antiferromagnetic exchange of  $J \approx 220 - 250$  K. The origin of the spin liquid phase is unresolved since the geometrical frustration introduced by a triangular lattice should not be sufficient to stabilize the quantum spin liquid state for ordinary Heisenberg exchange interactions [23–25]. Recently it was proposed that, alternatively, intrinsic disorder [26–28] or dynamical fluctuations [29] may play a crucial role for stabilizing the spin-liquid state in these molecular materials.

In contrast to the completely insulating material Herbertsmithite, where the on-site Coulomb repulsion  $U$  and bandwidth  $W$  are in the eV range ( $U = 8$  eV [31]), the energy scales of these organic compounds are significantly smaller; here, cooling from 300 K has a large effect on the Mott gap and the dc conductivity can be measured over the entire temperature range [22, 28, 30]. Moreover, the molecular conductors under study are closer to the metallic phase due to weaker correlations. With  $U/W \approx 1.5$ , CuCN is almost at the metal-insulator transition; in fact it becomes superconducting at  $T_c = 3.6$  K under hydrostatic pressure of only 4 kbar [7] or 12% BEDT-STF substitution [32]. For AgCN the effective correlations are more pronounced, as  $U/W = 2$ , while EtMe is far on the Mott insulating side with  $U/W \approx 2.4$  [33]. Heat capacity measurements suggested gapless spin excitations for CuCN [34], in contrast to thermal transport data [35]. For EtMe both thermodynamic probes [36, 37] and magnetization data [38] favor a gapless scenario whereas NMR results indicate a nodal spin gap [39].

A possible scenario featuring gapless spin excitations has been proposed by Lee and by collaborators [40], based on a U(1) gauge theory of the Hubbard model, suggesting a spinon Fermi surface, which should produce metallic-like low temperature behavior of both the specific heat and the thermal conductivity. In addition, the

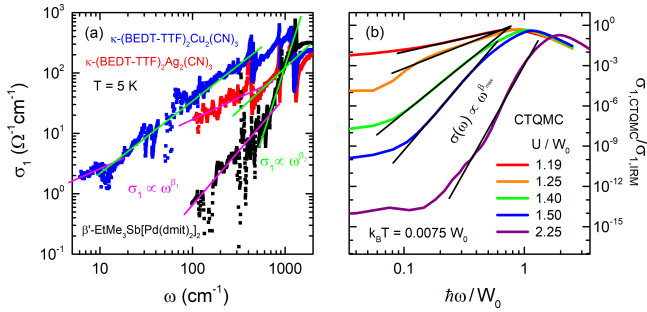


FIG. 1: (a) The in-gap conductivity of  $\beta'$ -EtMe<sub>3</sub>Sb[Pd(dmit)<sub>2</sub>]<sub>2</sub>,  $\kappa$ -(BEDT-TTF)<sub>2</sub>Ag<sub>2</sub>(CN)<sub>3</sub> and  $\kappa$ -(BEDT-TTF)<sub>2</sub>Cu<sub>2</sub>(CN)<sub>3</sub> can be approximated by power laws, as indicated by the straight lines in the double-logarithmic plot. Two different exponents are identified in different frequency regions. (b) Optical conductivity calculated by dynamical mean-field theory methods employing the continuous time quantum Monte Carlo (CTQMC) quantum impurity solver for different correlation strength  $U/W$  as indicated. The assumed  $k_B T/W = 0.0075$  corresponds to the low-temperature limit of our experiments.  $\sigma_1(\omega)$  is normalized to the Ioffe-Regel-Mott limit  $\sigma_{\text{IRM}}$ . Consistently, the exponents increase with correlation strength.

coupling of such spinons with an internal gauge field has been predicted to contribute to the optical conductivity [12, 41, 42] and even produce the magneto-optical Faraday effect [43]. This intriguing possibility motivated our present investigations on the electrodynamic behavior of quantum spin liquids. Deep within the Mott insulating state, where charge excitations are largely frozen out, we find signatures of a novel low-energy absorption band, which we attribute to anomalous excitations arising from the spin-disordered ground state in absence of antiferromagnetism.

From the general point of view, optical experiments are not sensitive to conventional spin excitations; however, spin-charge interactions may contribute to the low-energy optical conductivity, as suggested in theories featuring an emergent gauge field within the spin-liquid state [42, 44]. This mechanism was predicted to produce a power-law behavior:  $\sigma_1(\omega) \propto \omega^\beta$  with  $\beta = 2$  at low frequencies and a crossover to  $\beta = 3.3$  above  $\hbar\omega_c \approx k_B T$ . THz investigations on the kagome crystal ZnCu<sub>3</sub>(OH)<sub>6</sub>Cl<sub>2</sub> provided first experimental results [45] analyzed in this context: at  $T = 4$  K a power-law behavior of the optical conductivity was obtained with an exponent  $\beta = 1-2$  up to 1.4 THz when it crosses over into a phonon tail. There have been several attempts to investigate also the triangular compounds with a similar scope. Ng and Lee [42] analyzed the infrared spectra of CuCN, but the underlying data [46] do not extend to low-enough frequency to allow for reliable conclusions. Subsequent infrared reflectivity measurements by Elsässer *et al.* [47] could barely reach the relevant region around  $\hbar\omega \approx k_B T$  down to the lowest temperatures.

In order to provide more reliable data, we have compiled the electrodynamic properties of the dimer Mott insulators CuCN, AgCN and EtMe with quantum spin liquid ground states. The infrared optical reflectivity recorded by Fourier-transform spectroscopy over many orders of magnitude in frequency is supplemented by dc and dielectric studies in the kHz and MHz range and by ellipsometric measurements up to the ultraviolet in order to get more reliable extrapolations [22, 27, 28, 30, 33]. Fig. 1(a) displays the optical conductivity as obtained from the Kramers-Kronig analysis of the lowest-temperature data measured along the most conducting axes of CuCN, AgCN and EtMe. For light polarized along the second direction of the crystal surfaces, the overall behavior is rather similar [33, 48], indicating the two-dimensional electronic response despite a slight anisotropy. As indicated by the green and magenta lines, we can identify a power-law behavior  $\sigma_1(\omega) \propto \omega^{\beta_1}$  up to a crossover frequency  $\omega_c$  above which the slope approximately doubles. The exponents depend on temperature; in the case of CuCN, for instance, they start with  $\beta_1 \approx 0.4$  and  $\beta_2 \approx 0.8$  at  $T = 300$  K, and then increase to 0.9 and 1.3 upon cooling, respectively. While AgCN behaves rather similar as CuCN, the power-law exponents of EtMe are significantly larger, reaching  $\beta_1 = 1.75$  and  $\beta_2 = 4.2$  with a much more pronounced temperature dependence.

These observations can be explained by the increasing correlation strength  $U/W$  when going from CuCN to EtMe. While metallic fluctuations dominate the in-gap absorption of CuCN, a well-defined Mott gap forms only in EtMe upon cooling [33]. In order to investigate the correlation dependence of the steepness of the band edge, we calculated the optical spectra using Dynamical Mean-Field Theory (DMFT) utilizing the continuous time quantum Monte Carlo quantum impurity solver and plot the normalized spectra in Fig. 1(b). As expected, the Mott-Hubbard bands become more narrow and exhibit a steeper edge for enhanced  $U/W$ , very similar to the experimental spectra in panel (a) where the exponents are largest for the most strongly correlated compound EtMe. It should be stressed here that the DMFT approach, which focuses on local charge excitations, is not able to capture the relevant inter-site spin correlations contributing to spinon excitations. At this point we conclude that charge excitations, which are properly described by the DMFT theory, not only cause the mid-infrared band via transitions between the Hubbard bands, but also major parts of the sub-gap absorption with a power-law like increase in the optical range that levels off as the dc conductivity is approached.

Here we are in accord with recent theoretical results of Lee *et al.* [49], who concluded that long-lived spinon excitations are not well-defined close to the Mott transition. As soon as the electrons become delocalized, the spin has to follow the charge movement, which destroys

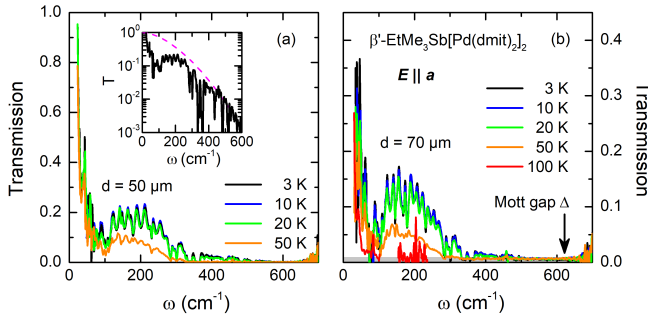


FIG. 2: Optical transmission spectra of  $\beta'$ -EtMe<sub>3</sub>Sb[Pd(dmit)<sub>2</sub>]<sub>2</sub> measured on two single crystals of (a) 50  $\mu\text{m}$  and (b) 70  $\mu\text{m}$  thickness at different temperatures. As the Mott gap opens below  $T \approx 125$  K, the transmission continuously increases down to the lowest temperatures. The sharp absorption features are due to molecular vibrations and lattice phonons, best identified in the semi-logarithmic plot of the inset. Pronounced Fabry-Perot oscillations appear at the lowest temperatures that allow to independently determine the real and imaginary parts of the conductivity with high accuracy. A broad absorption feature emerges below 200  $\text{cm}^{-1}$ . The power-law absorption  $\sigma_1(\omega) \propto \omega^{1.75}$  is indicated by a dashed pink line in the inset of panel (a) where a logarithmic scale is used.

the coherence of the postulated spinon Fermi surface. In other words, fingerprints of spinon excitations can only be expected in the optical properties when the low-energy charge response is strongly suppressed. Among the investigated materials, this is realized solely for EtMe which is located deep inside the Mott state with a well-defined gap [33]. Even then we have to look at small frequencies and temperatures well below the antiferromagnetic exchange coupling  $J \approx 250$  K [20].

To that end, we have prepared two large EtMe single crystals as thin as 50 and 70  $\mu\text{m}$  and conducted optical transmission measurements in the low-energy range using coherent source and time domain THz spectrometers as well as Fourier-transform interferometers. As seen in Fig. 2, the specimens become successively more transparent below the Mott gap around 600  $\text{cm}^{-1}$  that opens when cooling below 125 K. Except of the known anisotropy, the overall behavior is similar for  $E \parallel b$ . Most important, there is a pronounced dip in the transmission centered around 100  $\text{cm}^{-1}$  that indicates a novel absorption mechanism discussed in the following.

The real and imaginary parts of the optical conductivity are directly calculated from the optical transmission and reflection data. This way, the sensitivity is greatly enhanced and any arbitrary extrapolation of data can be avoided. In addition, a fit of the well-defined Fabry-Perot oscillations below 400  $\text{cm}^{-1}$  allows us to independently extract the complex optical response from the transmission data only. The so-obtained conductivity is superimposed on the results from the Kramers-Kronig analysis of the optical reflectivity and plotted in Fig. 3 (a).

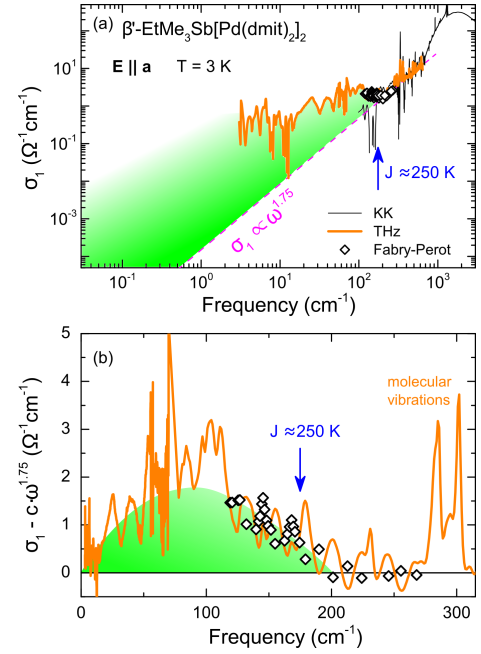


FIG. 3: (a) Low-temperature conductivity spectra of  $\beta'$ -EtMe<sub>3</sub>Sb[Pd(dmit)<sub>2</sub>]<sub>2</sub> plotted in a broad range. The black line corresponds to Kramers-Kronig results from optical reflectivity measurements; it is superimposed by the data directly calculated from transmission and reflection experiments in the THz and far-infrared ranges (orange). The open black diamonds are obtained from fits of the Fabry-Perot oscillations. The smooth behavior between 200 and 500  $\text{cm}^{-1}$  is described by a power-law  $\sigma_1(\omega) \propto \omega^{1.75}$  (dashed magenta line, cf. Figs. 1 and 2). As indicated in light green, the absorption exceeds the Mott-Hubbard band edge for frequencies below the antiferromagnetic exchange coupling  $J \approx 250$  K. (b) After subtracting the power-law background related with pure charge excitations, we obtain a broad low-energy feature below approximately 200  $\text{cm}^{-1}$ , which is close to the antiferromagnetic exchange energy of  $\beta'$ -EtMe<sub>3</sub>Sb[Pd(dmit)<sub>2</sub>]<sub>2</sub>. Hence, we associate the green dome-like area to low-energy excitations in the spin-liquid state. The narrow modes at higher frequencies correspond to vibrational features.

According to Fig. 1, the background conductivity of EtMe due to pure charge excitations is given by a power law  $\sigma_1(\omega) \propto \omega^{1.75}$  in the far-infrared range, where the tail of the Mott-Hubbard band dominates. At much lower energies it gradually levels off towards the dielectric and dc data, which are more than 10 orders of magnitude smaller than the THz conductivity at liquid He temperatures [28, 33]. Thus, the power-law behavior extrapolates down to audio and radio frequencies where the constant  $\sigma_{dc}$  is approached. In the range from 5 to 200  $\text{cm}^{-1}$  the absorption measured at  $T = 3$  K significantly exceeds this electronic background, as indicated in Fig. 3 (a). At the lowest measured frequency (3  $\text{cm}^{-1}$ ) this extra contribution is more than two orders of magnitude larger than the contribution from charge excitations and, thus, constitutes the main part of the optical conductivity. It is

important to note, however, that also this novel absorption channel decays towards low frequencies, although initially not as quickly as the charge response.

In order to unravel the nature of the exotic in-gap excitations, we subtract the  $\omega^{1.75}$  power-law and thus eliminate the electronic background. Since the charge contribution is much smaller, this phenomenological procedure does not affect the low-energy part, revealing the dome-like band plotted in Fig. 3 (b) which peaks slightly below  $100 \text{ cm}^{-1}$ . Apart from a few small phononic features on top, the band is rather isotropic and confined to a frequency range comparable to the antiferromagnetic exchange energy  $J \approx 250 \text{ K} = 175 \text{ cm}^{-1}$ . Thus, we may assign this dome-shaped in-gap absorption to spin excitations which occur when  $J$  is the dominant energy scale and the electronic conductivity is sufficiently suppressed at low temperatures.

In the measured range we do not find any indications of the power laws predicted by Lee and collaborators [40, 42]. Still, our data do not rule out  $\omega^2$  behavior at lower frequency, which would be consistent with the observed decay towards zero energy: in the static limit  $\sigma_1(\omega)$  decays faster than the  $\omega^{1.75}$  power-law background of the charge excitations. In this case, spinons affect neither the optical range nor the dc response where the physics of correlated electrons prevails; they may be observed at finite temperatures in a limited frequency range well below the Mott gap.

Another way to scrutinize the broadband spin response is via magnetic scattering techniques. While neutron scattering can map the dispersion relation of magnetic excitations [1], Raman spectroscopy is sensitive to the spin degrees of freedom only via higher-order excitations, such as two-magnon processes [3, 50]. A sharp resonance is observed in antiferromagnets due to well-defined magnon energies. In quantum spin liquids, however, the absence of magnetic order gives rise to broad scattering features, commonly interpreted as the creation of a pair of spinons for each magnon [1]. Indeed, such Raman signatures were observed in EtMe, AgCN and CuCN [51–53], as well as in the inorganic kagome and honeycomb materials Herberthsmithite [54] and  $\alpha\text{-RuCl}_3$  [55], respectively. The latter report even points out the putative fermionic behavior of the magnetic continuum at low temperatures. It is interesting to note that the Raman feature of EtMe is centered around  $400 \text{ cm}^{-1}$  [51] which is almost exactly four times larger than the peak position of the band observed here (Fig. 3). Considering that a two-magnon process is equivalent to four spin- $\frac{1}{2}$  excitations, one might speculate whether spin-charge coupling directly maps spinons via the charge response. Spectroscopic studies under magnetic field may elucidate the nature of these low-energy excitations [43].

Although an assignment of the low-frequency band (Fig. 3) to spin- $\frac{1}{2}$  excitations seems plausible, we discuss other possible sources of low-energy absorption. Con-

sidering the rather extended width of  $\approx 100 \text{ cm}^{-1}$  we can certainly rule out a simple phononic origin; typical vibrations have a width of  $5\text{--}10 \text{ cm}^{-1}$ . A recent pressure-dependent NMR and transport study revealed the importance of intrinsic disorder for the slow dynamics of EtMe [56]; still, it is unlikely that disorder alone contributes to the electrodynamic response at THz frequencies. Having in mind the broadening effect of spin excitations via magneto-elastic coupling [57], phononic processes combined with disorder may map the magnetic excitations to the electrodynamic response. Yet, the comparably strong oscillator strength of our data favors more a direct excitation process, e.g. via spin-charge interactions.

Going back to the overview on several quantum spin liquids plotted in Fig. 1, we can now understand why for CuCN no indications of magnetic excitations could be seen in the optical conductivity [46–48]. Due to the weaker correlations  $U/W$  the compound is located much closer to the insulator-metal phase boundary [33] and consequently the tail of the Mott-Hubbard excitations decays much slower towards  $\omega \rightarrow 0$ , as depicted in Fig. 1(b). CuCN exhibits a power-law conductivity with a weaker slope ( $\beta_{1,2} = 0.4\text{--}0.8$ ) and larger absolute value compared to EtMe. Hence, the electronic contribution to the electrodynamic response of CuCN dominates well into the GHz range of frequency.

From our comprehensive studies of three organic compounds with a triangular lattice we learnt that the large electronic conductivity even below the Mott-Hubbard gap makes it difficult to identify electronic excitations of the quantum-spin-liquid state. Only when investigating the strongly correlated Mott insulator  $\beta'\text{-EtMe}_3\text{Sb-[Pd(dmit)}_2\text{]}_2$  at very low frequencies and temperatures, we succeeded identifying an excess conductivity that cannot be explained by the charge response of the correlated electrons. Upon subtracting their smooth power-law background, a broad mode is identified delimited by  $J$  at its high-energy end; the strong decrease for  $\omega \rightarrow 0$  is consistent with the  $\omega^2$  dependence expected for spinons. This result is in excellent agreement with the recent picture based on a spinon-extension of dynamical mean field theory [49], which argue that the controversially discussed spinon Fermi surface melts away upon approaching the Mott metal-insulator transition. As soon as the electrons start moving as a whole, spin-charge separation is lost and the spin excitations are not independent from the charge motion any more. We suggest that it is worth turning back to Herberthsmithite and its recently synthesized analogues [58, 59], which exhibit a more pronounced charge gap [31], and investigate these strongly correlated compounds on a kagome lattice at extremely low temperatures and frequencies.

We thank P.A. Lee, S. Tomic and R. Valentí for valuable discussions. The project was supported by the Deutsche Forschungsgemeinschaft (DFG, grant

DR228/39-1) and the Russian Ministry of Education and science (Program 5 top 100). R. K. was supported in part by the Japan Society for the Promotion of Science Grants-in-Aid for Scientific Research (grant No. 16H06346). T.-H. L. and V. D. were partially supported by the NSF grant DMR-1410132.

---

[1] L. Balents, *Nature* **464**, 199 (2010).

[2] M. R. Norman, *Rev. Mod. Phys.* **88**, 041002 (2016).

[3] L. Savary and L. Balents, *Rep. Progr. Phys.* **80**, 016502 (2017).

[4] Y. Zhou, Kanoda, and T. K. Ng, *Rev. Mod. Phys.* **89**, 025003 (2017).

[5] I. Y. Pomeranchuk, *Zh. Eksp. Teor. Fiz.* **11**, 226 (1941).

[6] P. W. Anderson, *Mater. Res. Bull.* **8**, 153 (1973).

[7] Y. Shimizu, K. Miyagawa, K. Kanoda, M. Maesato, and G. Saito, *Phys. Rev. Lett.* **91**, 107001 (2003); Y. Kurosaki, Y. Shimizu, K. Miyagawa, K. Kanoda, and G. Saito, *Phys. Rev. Lett.* **95**, 177001 (2005).

[8] M. P. Shores, E. A. Nytko, B. M. Bartlett, and D. G. Nocera, *J. Am. Chem. Soc.* **127**, 13 462 (2005).

[9] J. S. Helton, K. Matan, M. P. Shores, E. A. Nytko, B. M. Bartlett, Y. Yoshida, Y. Takano, A. Suslov, Y. Qiu, J.-H. Chung, D. G. Nocera, and Y. S. Lee, *Phys. Rev. Lett.* **98**, 107204 (2007).

[10] P. Mendels, F. Bert, M. A. de Vries, A. Olariu, A. Harrison, F. Duc, J. C. Trombe, J. S. Lord, A. Amato, and C. Baines, *Phys. Rev. Lett.* **98**, 077204 (2007).

[11] S. Yan, D. Huse, and S. White, *Science* **332**, 1173 (2011).

[12] A. C. Potter, T. Senthil, and P. A. Lee, *Phys. Rev. B* **87**, 245106 (2013).

[13] X.-G. Wen, *Phys. Rev. B* **65**, 165113 (2002).

[14] D. N. Sheng, O. I. Motrunich, and M. P. A. Fisher, *Phys. Rev. B* **79**, 205112 (2009).

[15] V. Kalmeyer and R. B. Laughlin, *Phys. Rev. Lett.* **59**, 2095 (1987); G. Misguich, C. Lhuillier, B. Bernu, and C. Waldtmann, *Phys. Rev. B* **60**, 1064 (1999).

[16] Y. Qi, C. Xu, and S. Sachdev, *Phys. Rev. Lett.* **102**, 176401 (2009); *ibid.* **102**, 189903 (2009).

[17] R. V. Mishmash, J. R. Garrison, S. Bieri and C. Xu, *Phys. Rev. Lett.* **111**, 157203 (2013).

[18] O. I. Motrunich, *Phys. Rev. B* **72**, 045105 (2005).

[19] Y. Ran, M. Hermele, P. A. Lee, and X.-G. Wen, *Phys. Rev. Lett.* **98**, 117205 (2007).

[20] T. Itou, A. Oyamada, S. Maegawa, M. Tamura, and R. Kato, *Phys. Rev. B* **77**, 104413 (2008); T. Itou, A. Oyamada, S. Maegawa, and R. Kato, *Nature Phys.* **6**, 673 (2010).

[21] Y. Shimizu, T. Hiramatsu, M. Maesato, A. Otsuka, H. Yamochi, A. Ono, M. Itoh, M. Yoshida, M. Takigawa, Y. Yoshida, G. Saito, *Phys. Rev. Lett.* **117**, 107203 (2016).

[22] M. Pinterić, P. Lazić, A. Pustogow, T. Ivetk, M. Kuveždić, O. Milat, B. Gumhalter, M. Basletić, M. Čulo, B. Korin-Hamzić, A. Löhle, R. Hübner, M. Sanz Alonso, T. Hiramatsu, Y. Yoshida, G. Saito, M. Dressel, and S. Tomić, *Phys. Rev. B* **94**, 161105(R) (2016).

[23] D. A. Huse and V. Elser, *Phys. Rev. Lett.* **60**, 2531 (1988).

[24] L. Capriotti, A. E. Trumper, and S. Sorella, *Phys. Rev. Lett.* **82**, 3899 (1999).

[25] R. Kaneko, S. Morita, and M. Imada, *J. Phys. Soc. Jpn.* **83**, 093707 (2014).

[26] T. Furukawa, K. Miyagawa, T. Itou, M. Ito, H. Taniguchi, M. Saito, S. Iguchi, T. Sasaki, and K. Kanoda, *Phys. Rev. Lett.* **115**, 077001 (2015).

[27] M. Dressel, P. Lazić, A. Pustogow, E. Zhukova, B. Gorshunov, J. A. Schlueter, O. Milat, B. Gumhalter, and S. Tomić, *Phys. Rev. B* **93**, 081201 (2016).

[28] P. Lazić, M. Pinterić, D. R. Góngora, A. Pustogow, K. Treptow, T. Ivetk, O. Milat, B. Gumhalter, N. Došlić, M. Dressel, and S. Tomić, *arXiv:1710.01942*

[29] T. Yamamoto, T. Fujimoto, T. Naito, Y. Nakazawa, M. Tamura, K. Yakushi, Y. Ikemoto, T. Moriwaki, and R. Kato, *Sci. Rep.* **7**, 12930 (2017).

[30] M. Pinterić, M. Čulo, O. Milat, M. Basletić, B. Korin-Hamzić, E. Tafra, A. Hamzić, T. Ivetk, T. Peterseim, K. Miyagawa, K. Kanoda, J. A. Schlueter, M. Dressel, and S. Tomić, *Phys. Rev. B* **90**, 195139 (2014).

[31] A. Pustogow, Y. Li, I. Voloshenko, P. Puphal, C. Krellner, I.I. Mazin, M. Dressel, and R. Valentí, *Phys. Rev. B* **96**, 241114(R) (2017).

[32] A. Pustogow, A. Löhle, Y. Saito, Y. Ihara and A. Kawamoto, and M. Dressel, to be published

[33] A. Pustogow, M. Bories, A. Löhle, R. Rösslhuber, E. Zhukova, B. Gorshunov, S. Tomić, J.A. Schlueter, R. Hübner, T. Hiramatsu, Y. Yoshida, G. Saito, R. Kato, T.-H. Lee, V. Dobrosavljević, S. Fratini and M. Dressel, *arXiv:1710.07241*

[34] S. Yamashita, Y. Nakazawa, M. Oguni, Y. Oshima, H. Jojiri, K. Miyagawa, and K. Kanoda, *Nature Phys.* **4**, 459 (2008).

[35] M. Yamashita, N. Nakata, Y. Kasahara, T. Sasaki, N. Yoneyama, N. Kobayashi, S. Fujimoto, T. Shibauchi, and Y. Matsuda, *Nature Phys.* **5**, 44 (2009).

[36] S. Yamashita, T. Yamamoto, Y. Nakazawa, M. Tamura, and R. Kato, *Nat. Commun.* **2**, 275/1-275/6 (2011).

[37] M. Yamashita, N. Nakata, Y. Senshu, M. Nagata, H. M. Yamamoto, R. Kato, T. Shibauchi, and Y. Matsuda, *Science* **328**, 1246 (2010).

[38] D. Watanabe, M. Yamashita, S. Tonegawa, Y. Oshima, H. M. Yamamoto, R. Kato, I. Sheikin, K. Behnia, T. Terashima, S. Uji, T. Shibauchi, and Y. Matsuda, *Nat. Commun.* **3**, 1090 (2012).

[39] T. Itou, A. Oyamada, S. Maegawa, and R. Kato, *Nat. Phys.* **6**, 673 (2010).

[40] S.-S. Lee and P.A. Lee, *Phys. Rev. B* **72**, 235104 (2005); S.-S. Lee, P. A. Lee, and T. Senthil, *Phys. Rev. Lett.* **98**, 067006 (2007).

[41] L. B. Ioffe and A. I. Larkin, *Phys. Rev. B* **39**, 8988 (1989).

[42] T.-K. Ng and P. A. Lee, *Phys. Rev. Lett.* **99**, 156402 (2007).

[43] J. R. Colbert, H. D. Drew, and P. A. Lee, *Phys. Rev. B* **90**, 121105 (2014).

[44] Y. Zhou and T.-K. Ng, *Phys. Rev. B* **88**, 165130 (2013); Y.-F. Ma and T.-K. Ng, *arXiv: 1410.6330*.

[45] D. V. Pilon, C. H. Lui, T. -H. Han, D. Shrekenhamer, A. J. Frenzel, W. J. Padilla, Y. S. Lee, and N. Gedik, *Phys. Rev. Lett.* **111**, 127401 (2013).

[46] I. Kezsmárki, Y. Shimizu, G. Mihaly, Y. Tokura, K. Kanoda, and G. Saito, *Phys. Rev. B* **74**, 201101 (2006).

[47] S. Elsässer, D. Wu, M. Dressel, and J. A. Schlueter, *Phys. Rev. B* **86**, 155150 (2012).

[48] A. Pustogow, E.Zhukova, B. Gorshunov, M. Pinterić, S. Tomić, J. A. Schlueter and M. Dressel, *arXiv:1412.4581*

- [49] T.-H. Lee, S. Florens, and V. Dobrosavljević, Phys. Rev. Lett. **117**, 136601 (2016).
- [50] W. Weber and R. Merlin, *Raman Scattering in Materials Science* (Springer Science & Business Media, 2000).
- [51] Y. Nakamura, R. Kato, H. Kishida, J. Phys. Soc. Jpn. **84**, 44715 (2015).
- [52] Y. Nakamura, N. Yoneyama, T. Sasaki, T. Tohyama, A. Nakamura and H. Kishida, J. Phys. Soc. Jpn. **83**, 74708 (2014).
- [53] Y. Nakamura, T. Hiramatsu, Y. Yoshida, G. Saito and H. Kishida, J. Phys. Soc. Jpn. **86**, 14710 (2016).
- [54] D. Wulferding, P. Lemmens, P. Scheib, J. Röder, P. Mendels, S. Chu, T. Han, and Y. S. Lee, Phys. Rev. B **82**, 144412 (2010).
- [55] L. J. Sandilands, Y. Tian, K. W. Plumb, Y.-J. Kim, and K. S. Burch, Phys. Rev. Lett. **114**, 147201 (2015).
- [56] T. Itou, E. Watanabe, S. Maegawa, A. Tajima, N. Tajima, K. Kubo, R. Kato, and K. Kanoda, Sci. Adv. **3**, e1601594 (2017).
- [57] A. B. Sushkov, G. S. Jenkins, T.-H. Han, Y. S. Lee, and H. D. Drew, J. Phys.: Condens. Matter **290**, 095802 (2017).
- [58] W. Sun, Y.-X. Huang, S. Nokhrin, Y. Pan and J.-X. Mi, J. Mater. Chem. C **4**, 8772 (2016).
- [59] P. Puphal, M. Bolte, D. Sheptyakov, A. Pustogow, K. Kliemt, M. Dressel, M. Baenitz, and C. Krellner, J. Mater. Chem. C **5**, 2629 (2017).